Multimode Network Description of a Planar Periodic Metal-Strip Grating at a Dielectric Interface—Part III: Rigorous Solution

MARCO GUGLIELMI AND HARRY HOCHSTADT

Abstract —In a recent pair of papers we studied the scattering problem posed by a plane wave incident at an angle on a plane, periodic, metal-strip grating at a dielectric interface. In the first paper (Part I) we formulated the solution to the scattering problem in terms of *novel multimode equivalent network representations.* The analytical phrasing followed in Part I led to two Fredholm integral equations of the first kind with singular kernels. In the second paper (Part II) we presented two approximate solution procedures for those integral equations that led to four simple and accurate equivalent network representations for the scattering problem under investigation. In this paper (Part III) we further this investigation by deriving a *novel rigorous analytical solution* for one of the two integral equations derived in Part I. We obtain closed-form, rigorous, analytical expressions for the elements involved in the equivalent network representations derived. Finally, we present the results of a number of numerical computations carried out by using the rigorous equivalent networks developed.

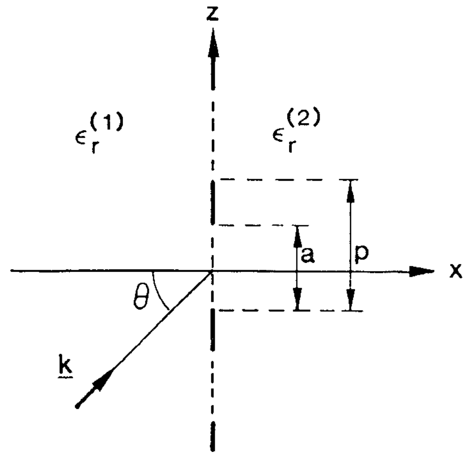

Fig 1. The structure under investigation is a zero-thickness metal-strip grating at a plane dielectric interface. The excitation is a plane wave at an angle; both TE and TM polarizations are considered. The ratio between the period p and the wavelength λ_0 of the incident plane wave is such that higher propagating modes (spectral orders) must be explicitly considered.

I. Introduction

IN A RECENT pair of papers [1], [2] we presented novel small-aperture and small obstacle multimode equivalent network representations for the scattering problem posed by a plane wave incident on the plane, periodic, zero-thickness, metal-strip grating at a dielectric interface shown in Fig. 1. The problem was posed for both TE and TM incident modes and followed two different approaches, namely, the obstacle and the aperture approach, thereby yielding four different formulations. Solutions were first derived formally [1] in terms of shunt multimode coupling networks containing a coupling matrix whose generic elements $A_{m,n}$ were obtained, via an integral relation, from the solution of four integral equations. It was further shown [1] that to solve all four problems we only needed to solve two types of integral equations. These integral equations were then solved in [2] in the small argument limit, thereby giving four very accurate and simple novel multimode equivalent network representations for the multimode grating under investigation.

Manuscript received April 11, 1988; revised November 7, 1988.
M. Guglielmi was with the Department of Electrical Engineering, Polytechnic University, Brooklyn, NY. He is now with the European Space Research and Technology Centre, Noordwijk, The Netherlands.
H. Hochstadt is with the Department of Mathematics, Polytechnic University, 333 Jay Street, Brooklyn, NY 11201.
IEEE Long Number 8826584.

In this paper, we further this investigation by deriving a *novel* rigorous analytical solution for one of the two integral equations derived in [1], thereby obtaining two *rigorous equivalent network representations* for the multimode grating at a dielectric interface shown in Fig. 1. We present numerical results obtained by using these rigorous equivalent network representations for TE-mode and TM-mode incidence for the case in which the same dielectric is present on both sides of the grating as well as for the case in which the two dielectric media are different.

The rigorous results derived here, once employed in the network formulation presented in [1], yield two rigorous equivalent network representations. These networks, one for TM-mode and the other for TE-mode incidence, are valid for an arbitrary angle of incidence, an arbitrary value of the relative aperture size a/p in Fig. 1, arbitrary values of relative permittivity ϵ_r of the medium on each side of the grating, and an arbitrary number of propagating higher modes. They provide very general rigorous multimode equivalent network representations for the plane, periodic,

0018-9480/89/0500-0902$01.00 ©1989 IEEE

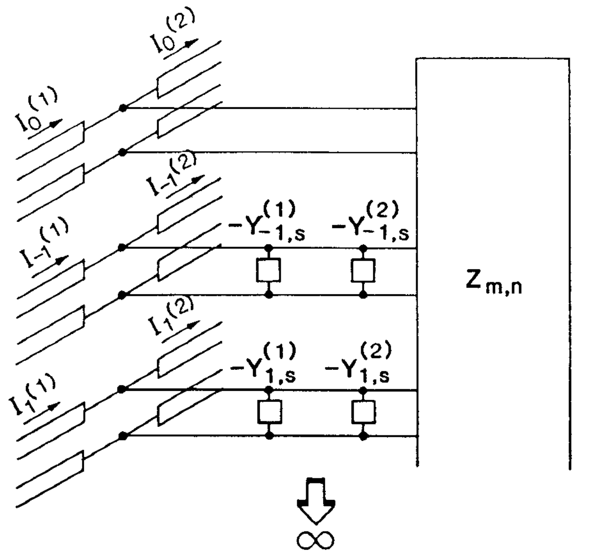

Fig. 2. Using the aperture formulation and TE-mode incident wave, we derived in [1] this formal network phrasing for the solution of the scattering problem shown in Fig. 1

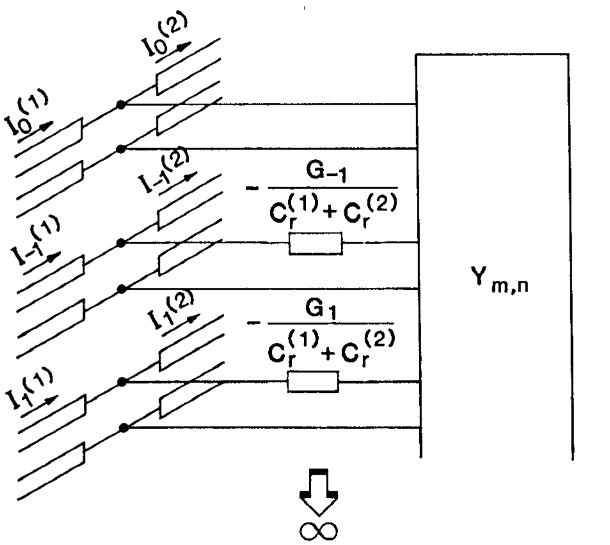

Fig. 3. Using the obstacle formulation and TM-mode incident wave, we derived in [1] this formal network phrasing for the solution of the scattering problem shown in Fig. 1.

metal-strip grating at a dielectric interface shown in Fig. 1. The value of these equivalent network representations lies in the fact that they can be used as constituent parts of equivalent network representations of more complex structures containing gratings of the type shown in Fig. 1.

II. The Equivalent Networks and the Relevant Singular Integral Equation

It is appropriate at this point to recall the results of the formal rigorous network phrasing derived in [1] for the scattering problem under investigation. In Figs. 2 and 3 we show the equivalent network representations derived for the cases of TE-mode incident wave and aperture formulation and for TM-mode incident wave and obstacle formulation, respectively. The quantities defined in Figs. 2 and 3 are given by

$$C_r^{(m)} = \epsilon_r^{(m)} \tag{1}$$

$$G_n = \frac{2\pi|n|}{j\omega\epsilon_0 p} \tag{2}$$

$$Y_{n,s}^{(m)} = \frac{2\pi|n|}{j\omega\mu_0\mu_r^{(m)} p} \tag{3}$$

$$A_{m,n} = \int_D f_n(z) e^{j\frac{2m\pi}{p}z} dz \tag{4}$$

where the coupling coefficient $A_{m,n}$ represents $Z_{m,n}$ in Fig. 2 if the domain of integration D extends over the aperture in Fig. 1 $(-a/2 \leqslant z \leqslant a/2)$ or represents $Y_{m,n}$ in Fig. 3 if the domain of integration D extends over the obstacle and the origin of the coordinate system is shifted to the center of a metal strip so that $-(p-a)/2 \leqslant z \leqslant (p-a)/2$. Note that the element $Y_{n,s}^{(m)}$ in (3) is the static characteristic admittance for TE modes, as defined in [1, eq. (4)]. The superscript (m) in (1) and (3) takes the value 1 or 2 to indicate the medium to the left of the grating or the one to the right, respectively.

The unknown function $f_n(z)$ in (4) is specified via the singular integral equation

$$e^{-j\frac{2n\pi}{p}z} = \int_D f_n(z') B \sum_{m \neq 0} |m| e^{-j\frac{2m\pi}{p}(z-z')} dz' \tag{5}$$

where the same convention is used for the domain of integration D, and the constant B is given by

$$B = \begin{cases} \dfrac{2\pi}{j\omega\epsilon_0 p} \dfrac{1}{\epsilon_r^{(1)} + \epsilon_r^{(2)}} & \text{for TM-mode excitation} \\ \dfrac{2\pi}{j\omega\mu_0 p} \left[\dfrac{1}{\mu_r^{(1)}} + \dfrac{1}{\mu_r^{(2)}} \right] & \text{for TE-mode excitation.} \end{cases} \tag{6}$$

III. Rigorous Analytical Expressions for the Multimode Coupling Matrix Coefficients

To derive a rigorous analytical expression for $A_{m,n}$ in (4) we must first solve the singular integral equation in (5). To do so, we first rewrite its kernel in the form

$$K(z-z') = \lim_{\delta \to 0} \sum_{m \neq 0} |m| e^{-\delta|m|} e^{-j\frac{2m\pi}{p}(z-z')} \tag{7}$$

to aid in summing the kernel in closed form. This phrasing is in principle equivalent to formulating the integral equation a small distance δ away from the grating in the x direction and then taking the limit for $\delta \to 0$. Next, we substitute (7) into (5) and, integrating by parts, obtain

$$e^{-j\frac{2n\pi}{p}z} = \int_{-b/2}^{b/2} f_n'(z') \frac{B}{-j\dfrac{2\pi}{p}} \cdot \lim_{\delta \to 0} \sum_{m \neq 0} \frac{|m|}{m} e^{-\delta|m|} e^{-j\frac{2m\pi}{p}(z-z')} dz' \tag{8}$$

together with the condition

$$f_n(z')\big|_{z' = \pm b/2} = 0 \tag{9}$$

where $\pm b/2$ are the end points of the domain of integration D previously defined. The kernel of (8) can now be summed in closed form by recalling that [3]

$$\sum_{m=1}^{\infty} e^{-\delta m} \sin mx = \frac{1}{2} \frac{\sin x}{\cosh\delta - \cos x}. \quad (10)$$

Taking the limit for $\delta \to 0$ we can finally express (8) in the more convenient form

$$e^{-j\frac{2n\pi}{p}z} = \int_{-b/2}^{b/2} f_n'(z') \frac{Bp}{2\pi} \frac{\sin\frac{2\pi}{p}(z-z')}{1-\cos\frac{2\pi}{p}(z-z')} dz'. \quad (11)$$

Next, using the double angle formulas, we rewrite (11) in the form

$$e^{-jn\pi\frac{b}{p}x} = \int_{-1}^{1} f'_n\left(\frac{b}{2}x'\right) \frac{Bpb}{4\pi} \cot\frac{\pi}{2}\frac{b}{p}(x-x')\, dx' \quad (12)$$

where we have also used the changes of variables

$$z = \frac{b}{2}x \quad (13)$$

$$z' = \frac{b}{2}x'. \quad (14)$$

Equation (12) is a singular integral equation of the Hilbert type that has a known inversion formula only for the special case $b/p = 1.0$ [4]. A new solution is, therefore, needed in this case since b/p is less than unity. We refer the reader to Appendix I for the mathematical details of the derivation of the *novel rigorous* solution of (12) and present here only the final results by writing the solution of (12) in the form

$$F_n(\alpha\eta) = \frac{1}{\sqrt{1-\eta^2}}\left[C_2 + I_n^{(1)}(\alpha\eta) + C_1\eta\right] \quad (15)$$

where

$$F_n(\alpha\eta) = f_n'\left[\frac{p}{\pi}\tan^{-1}(\alpha\eta)\right]\frac{Bp^2}{2\pi} \quad (16)$$

$$\tan\frac{\pi}{2}\frac{b}{p}x = \alpha\eta \quad (17)$$

$$\alpha = \tan\frac{\pi}{2}\frac{b}{p} \quad (18)$$

$$I_n^{(1)}(\alpha\eta) = \frac{1}{\pi} \fint_{-1}^{1} \frac{\sqrt{1-\xi^2}}{\xi-\eta} g_n(\alpha\xi)\, d\xi \quad (19)$$

$$g_n(\alpha\eta) = e^{-j2n\tan^{-1}\alpha\eta} \quad (20)$$

$$C_1 = \frac{\hat{D}_n}{\tilde{D}} \quad (21)$$

$$\hat{D}_n = \int_{-1}^{1} \frac{\eta I_n^{(1)}(\alpha\eta)}{\sqrt{1-\eta^2}\left[1+(\alpha\eta)^2\right]} d\eta \quad (22)$$

$$\tilde{D} = \frac{\pi}{\alpha^2} - \int_{-1}^{1} \frac{\eta^2}{\sqrt{1-\eta^2}\left[1+(\alpha\eta)^2\right]} d\eta. \quad (23)$$

The constant C_2 in (15) is an arbitrary constant to be evaluated later. The star on the integral sign in (19) means that we take its principal value.

Now that we have the rigorous solution of (12), we can proceed with the derivation of the analytical expression for the coupling coefficients $A_{m,n}$ defined in (4). Recalling (16), the relation between $F_n(\alpha\eta)$ and $f_n'(z)$, we can write

$$f_n\left[\frac{p}{\pi}\tan^{-1}(\alpha\eta)\right] = \frac{2\alpha}{pB}\int_{-1}^{\eta} \frac{F_n(\alpha\xi)}{\left[1+(\alpha\xi)^2\right]} d\xi \quad (24)$$

where we have already used the changes of variables given in (13) and (17).

To find an expression for constant C_2 in (15), can use (24) and condition (9) imposed earlier on $f_n(z)$, obtaining

$$C_2 = -\frac{D_n(1)}{D(1)} \quad (25)$$

where

$$D(\eta) = \int_{-1}^{\eta} \frac{d\xi}{\sqrt{1-\xi^2}\left[1+(\alpha\xi)^2\right]} \quad (26)$$

$$D_n(\eta) = \int_{-1}^{\eta} \frac{I_n^{(1)}(\alpha\xi)}{\sqrt{1-\xi^2}\left[1+(\alpha\xi)^2\right]} d\xi. \quad (27)$$

Using now (15) through (27) we can write

$$f_n\left[\frac{p}{\pi}\tan^{-1}(\alpha\eta)\right] = \frac{2\alpha}{Bp}\left[D_n(\eta) - \frac{D_n(1)}{D(1)}D(\eta) + \frac{\hat{D}_n}{\tilde{D}}\hat{D}(\eta)\right] \quad (28)$$

where the function $\hat{D}(\eta)$ is defined as

$$\hat{D}(\eta) = \int_{-1}^{\eta} \frac{\xi\, d\xi}{\sqrt{1-\xi^2}\left[1+(\alpha\xi)^2\right]}. \quad (29)$$

The final step is now to use (28) and (4), together with the necessary changes of variables, to derive an expression for the generic coupling matrix element $A_{m,n}$, obtaining

$$A_{m,n} = \frac{2\alpha^2}{\pi B}\left[D_{m,n} - \frac{D_m D_n}{D} + \frac{\hat{D}_m \hat{D}_n}{\tilde{D}}\right] \quad (30)$$

where

$$D = D(1) \quad (31)$$

$$D_n = D_n(1) \quad (32)$$

$$D_m = \int_{-1}^{1} \frac{I_m^{(2)}(\alpha\eta)}{\sqrt{1-\eta^2}\left[1+(\alpha\eta)^2\right]} d\eta \quad (33)$$

$$\hat{D}_m = \int_{-1}^{1} \frac{\eta I_m^{(2)}(\alpha\eta)}{\sqrt{1-\eta^2}\left[1+(\alpha\eta)^2\right]} d\eta \quad (34)$$

$$D_{m,n} = \int_{-1}^{1} \frac{I_m^{(2)}(\eta\alpha) I_n^{(1)}(\eta\alpha)}{\sqrt{1-\eta^2}\left[1+(\alpha\eta)^2\right]} d\eta \quad (35)$$

$$I_m^{(2)}(\alpha\eta) = \int_{\eta}^{1} \frac{g_m^*(\alpha\xi)}{\left[1+(\alpha\xi)^2\right]} d\xi \quad (36)$$

and the superscript $*$ means complex conjugate. Note that to obtain the expressions in (33), (34), and (35) we have performed an inversion of the order of integration.

The expression for the coupling coefficients $A_{m,n}$ that we have just derived can be written in a simpler form by recalling that, since the structure under examination is lossless, the coefficients $A_{m,n}$ must be imaginary. We can therefore separate the real from the imaginary parts of the terms inside the square brackets in (30), carry out the algebraic operations, and retain only the resulting real part since the coefficients D and $\hat{D}$ are real, and B is already purely imaginary, as shown in (6). In addition to that, as we show in Appendix II, it is possible to separate $I_n^{(1)}(\alpha\eta)$ and $I_m^{(2)}(\alpha\eta)$ into even and odd components, thus obtaining a simpler final expression for $A_{m,n}$. Furthermore, if we define the operator $\mathrm{EL}\{f(\sin\frac{\pi}{2}\phi)\}$ according to

$$\mathrm{EL}\left\{f\left(\sin\frac{\pi}{2}\phi\right)\right\} = \frac{\pi}{2}\int_{-1}^{1}\frac{f\left(\sin\frac{\pi}{2}\phi\right)}{\left[1+\alpha^2\sin^2\frac{\pi}{2}\phi\right]}\,d\phi \quad (37)$$

we finally obtain for $A_{m,n}$ the expression

$$A_{m,n} = \frac{2\alpha^2}{\pi B}\Bigg[EL\left\{I_{m,\mathrm{real}}^{(2)}I_{n,\mathrm{real}}^{(1)} - I_{m,\mathrm{imag}}^{(2)}I_{n,\mathrm{imag}}^{(1)}\right\} + \frac{1}{D}EL\left\{I_{m,\mathrm{imag}}^{(2)}\right\}EL\left\{I_{n,\mathrm{imag}}^{(1)}\right\} + \frac{1}{\tilde{D}}EL\left\{\eta I_{m,\mathrm{real}}^{(2)}\right\}EL\left\{\eta I_{n,\mathrm{real}}^{(1)}\right\}\Bigg] \quad (38)$$

where

$$I_{m,\mathrm{real}}^{(2)} = -\frac{1}{2\alpha m}\sin\left[2m\tan^{-1}\alpha\left(\sin\frac{\pi}{2}\phi\right)\right] \quad (39)$$

$$I_{0,\mathrm{real}}^{(2)} = -\frac{1}{\alpha}\tan^{-1}\alpha\left(\sin\frac{\pi}{2}\phi\right) \quad (40)$$

$$I_{m,\mathrm{imag}}^{(2)} = -\frac{1}{2\alpha m}\cos\left[2m\tan^{-1}\alpha\left(\sin\frac{\pi}{2}\phi\right)\right] \quad (41)$$

$$I_{0,\mathrm{imag}}^{(2)} = 0 \quad (42)$$

$$I_{n,\mathrm{real}}^{(1)} = \frac{1}{2}\int_{-1}^{1}\frac{\cos^2\frac{\pi}{2}\psi\cos\left[2n\tan^{-1}\left(\alpha\sin\frac{\pi}{2}\psi\right)\right] - \cos^2\frac{\pi}{2}\phi\cos\left[2n\tan^{-1}\left(\alpha\sin\frac{\pi}{2}\phi\right)\right]}{\sin\frac{\pi}{2}\psi - \sin\frac{\pi}{2}\phi}\,d\psi \quad (43)$$

$$I_{0,\mathrm{real}}^{(1)} = -\sin\frac{\pi}{2}\phi \quad (44)$$

$$I_{n,\mathrm{imag}}^{(1)} = \frac{1}{2}\int_{-1}^{1}\frac{\cos^2\frac{\pi}{2}\psi\sin\left[2n\tan^{-1}\left(\alpha\sin\frac{\pi}{2}\psi\right)\right] - \cos^2\frac{\pi}{2}\phi\sin\left[2n\tan^{-1}\left(\alpha\sin\frac{\pi}{2}\phi\right)\right]}{\sin\frac{\pi}{2}\psi - \sin\frac{\pi}{2}\phi}\,d\psi \quad (45)$$

$$I_{0,\mathrm{imag}}^{(1)} = 0 \quad (46)$$

$$D = \frac{\pi}{\sqrt{1+\alpha^2}} \quad (47)$$

$$\tilde{D} = \frac{\pi}{\alpha^2\sqrt{1+\alpha^2}}. \quad (48)$$

The analytical details involved in the derivation of (39) through (48) are reported in Appendix II.

The expression for $A_{m,n}$ given in (38) is therefore the *rigorous*, *analytical* form of the generic element of the multimode coupling matrices shown in Figs. 2 and 3. Note that to obtain numerical values from (38) we need to perform double integrations; they can be easily performed to an arbitrary degree of accuracy using one of the many numerical integration procedures that are available in the literature. For all of the numerical results shown in the next section, we have used a 96-point Gauss integration procedure [5].

IV. Numerical Results

The scattering problem studied in this paper has already been investigated by many authors. As a result, there are now available in the literature a number of alternative solution procedures (for instance [2]–[15] of Part I [1]), and some of these solutions do yield exact or very accurate numerical results. The objective of this paper, however, is not to present yet another solution to this scattering problem but to provide a *novel rigorous multimode equivalent network representation* for the grating in Fig. 1. This goal has already been achieved in the preceding section; however, for completeness we also include some of the scattering results obtained by using the novel equivalent networks developed here.

Fig. 4 shows the result of the first numerical computation, where the structure chosen is a self-reciprocal and symmetric grating ($a/p = 0.5$ and $\epsilon_r^{(1)} = \epsilon_r^{(2)} = 1.0$ in Fig. 1) and the angle of incidence θ is equal to zero. The quantity computed is the transmitted power in the lowest mode ($n = 0$ mode) versus the relative period p/λ_0, and the incident wave is TE with respect to the x direction in Fig. 1. The equivalent network used is the one shown in Fig. 2. The result shown in Fig. 4 has been obtained explicitly including in the multimode equivalent network of the grating the $n = 0, \pm 1, \pm 2, \pm 3, \pm 4$ modes. In the frequency range between $p/\lambda_0 = 0$ and $p/\lambda_0 = 1$ in Fig. 4 only the $n = 0$ mode is above cutoff in the x direction of Fig. 1. At $p/\lambda_0 = 1$ the $n = \pm 1$ modes begin to propagate, at $p/\lambda_0 = 2$ the $n = \pm 2$ begin propagating, and so on to

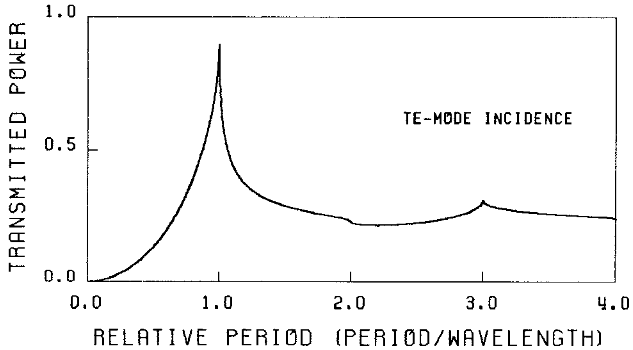

Fig. 4. Using the rigorous network shown in Fig. 2, we computed the transmitted power in the lowest mode ($n=0$ spectral order) versus the relative period p/λ_0 for TE-mode incidence on the structure in Fig. 1 with $a/p=0.5$, $\epsilon_r^{(1)}=\epsilon_r^{(2)}=1$, and $\theta=0$. In the computations we included explicitly modes of order up to $n=\pm 4$.

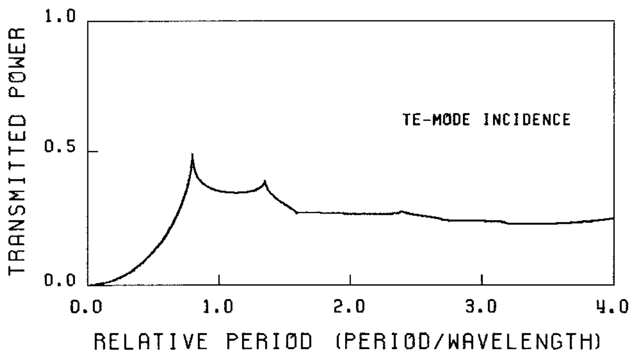

Fig. 5. Same as Fig. 4 but with the angle of incidence θ equal to 15°

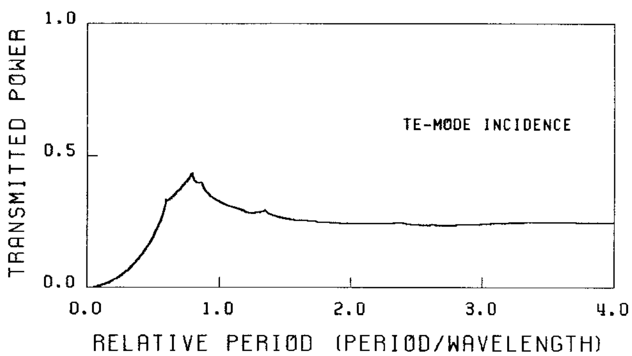

Fig. 6. Same as Fig. 5 but with $\epsilon_r^{(2)}=2.0$, and including explicitly in the equivalent network in Fig. 2 modes of the order up to $n=\pm 6$.

infinity. The general expression for the cutoff value of p/λ_0 in relation to the order of mode n is given by

$$\frac{p}{\lambda_0}=-\frac{\pm n}{\pm\sin\theta-\sqrt{\epsilon_r^{(m)}}} \tag{49}$$

where the plus sign is to be used for $n>0$ and the minus sign for $n<0$.

Changing the angle of incidence θ to 15° and keeping the rest unchanged, we have then obtained the result shown in Fig. 5. Furthermore, for the same value of θ but with $\epsilon_r^{(2)}=2.0$ we obtain the result shown in Fig. 6. In this last case, due to the presence of the different dielectric on one side of the grating, to adequately cover the same range

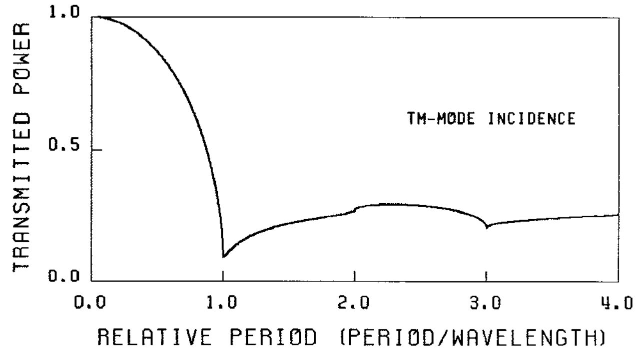

Fig. 7. Same as for Fig. 4 but for TM incidence. To obtain the results shown we have used the network in Fig 3.

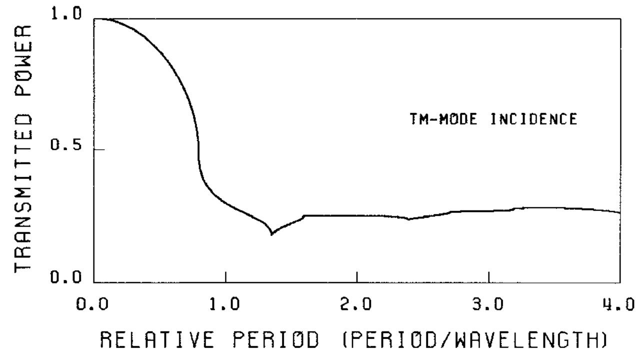

Fig. 8. Same as Fig. 5 but for TM incidence The network used is the one in Fig. 3

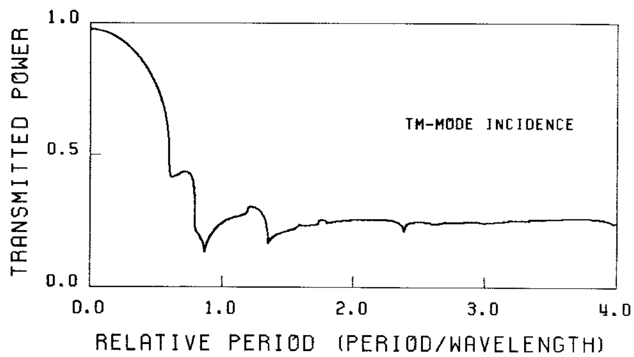

Fig. 9. Same as Fig. 6 but for TM incidence The network used is the one in Fig 3

of p/λ_0 we have explicitly included in the network representation of the grating transmission lines representing modes up to the order $n=\pm 6$.

In the next set of figures, namely Figs. 7, 8, and 9, we have used the same structures as in Figs. 4, 5, and 6, respectively, but for the case in which the incident plane wave has the magnetic field in the y direction of Fig. 1 (TM case). The network used in this case is the one shown in Fig. 3. Note that, as expected, the result shown in Fig. 7 appears to be exactly coincident with the rigorous result given by Baldwin and Heins [6] for the same structure.

Another feature of the results shown that is worth mentioning is that the results shown in Figs. 7 and 8 can be obtained computing the reflected power on the lowest mode for TE incidence instead of the transmitted power for TM incidence. This is a consequence of the duality principle and it does not apply to the result shown in Fig. 9. Finally, note that in Fig. 9 we observe that the transmitted power is less than unity in the limit of zero frequency. This is due to the fact that for a TM wave the value of the modal characteristic impedance changes as a function of the dielectric constant ϵ_r even in the limit of zero frequency. This, however, is not true for the TE case, as indicated in Fig. 6.

V. Conclusions

We have derived here a *novel* analytical inversion formula for Hilbert-type singular integral equations and *rigorous multimode equivalent network representations* for the scattering problem posed by a plane wave incident on the multimode, zero-thickness, metal-strip grating at a dielectric interface shown in Fig. 1. Both TE- and TM-mode excitations have been considered, thereby providing two rigorous multimode equivalent network representations that are valid at the same time for an arbitrary angle of incidence, different media on each side of the grating, and an arbitrary value of the relative aperture size a/p in Fig. 1. In addition to that, in the equivalent networks we have developed we can include explicitly an arbitrary number of propagating higher modes. Due to their generality, therefore, the equivalent networks developed are *powerful tools* for the analysis of more complex structures that contain the multimode metal strip grating shown in Fig. 1.

Appendix I

In this appendix we derive a *novel* inversion formula for (12) that is valid for arbitrary values of the parameter b/p that are less than unity. To do so, using the addition formulas, we first rewrite the kernel of (12) in the form

$$\cot\frac{\pi}{2}\frac{b}{p}(x-x') = \frac{\cot\frac{\pi}{2}\frac{b}{p}x\cot\frac{\pi}{2}\frac{b}{p}x'+1}{\cot\frac{\pi}{2}\frac{b}{p}x'-\cot\frac{\pi}{2}\frac{b}{p}x}. \tag{A1}$$

Next, we introduce the changes of variables

$$\tan\frac{\pi}{2}\frac{b}{p}x = \alpha\eta \tag{A2}$$

$$\tan\frac{\pi}{2}\frac{b}{p}x' = \alpha\eta' \tag{A3}$$

where

$$\alpha = \tan\frac{\pi}{2}\frac{b}{p}. \tag{A4}$$

Using now (A1) through (A4), we can rewrite (12) in the form

$$e^{-j2n\tan^{-1}\alpha\eta} = \int_{-1}^{1} f_n'\left(\frac{p}{\pi}\tan^{-1}\alpha\eta'\right) \cdot\frac{Bp^2}{2\pi^2}\left[\frac{1+\alpha^2\eta\eta'}{1+(\alpha\eta')^2}\right]\frac{d\eta'}{\eta-\eta'}. \tag{A5}$$

A key step toward the solution of (A5) is to rewrite the term inside the square brackets in the form

$$\frac{1+\alpha^2\eta\eta'}{1+(\alpha\eta')^2} = 1+\frac{\alpha^2\eta'}{1+(\alpha\eta')^2}(\eta-\eta') \tag{A6}$$

so that we can write

$$g_n(\alpha\eta) = \frac{1}{\pi}\int_{-1}^{1}\frac{F_n(\alpha\eta')}{\eta-\eta'}d\eta' + \frac{1}{\pi}\int_{-1}^{1}\frac{\alpha^2\eta' F_n(\alpha\eta')}{1+(\alpha\eta')^2}d\eta' \tag{A7}$$

where

$$F_n(\alpha\eta) = f_n'\left[\frac{p}{\pi}\tan^{-1}(\alpha\eta)\right]\frac{Bp^2}{2\pi} \tag{A8}$$

$$g_n(\alpha\eta) = e^{-j2n\tan^{-1}\alpha\eta}. \tag{A9}$$

Note that the second integral on the right-hand side of (A7) represents a constant. We can therefore define C_1 as

$$C_1 = \frac{1}{\pi}\int_{-1}^{1}\frac{\alpha^2\eta' F_n(\alpha\eta')}{1+(\alpha\eta')^2}d\eta' \tag{A10}$$

and write (A7) in the form

$$g_n(\alpha\eta) - C_1 = \frac{1}{\pi}\int_{-1}^{1}\frac{F_n(\alpha\eta')}{\eta-\eta'}d\eta'. \tag{A11}$$

Equation (A11) is a standard Cauchy-type singular integral equation of known solution [7]; we can therefore write

$$F_n(\alpha\eta) = \frac{1}{\sqrt{1-\eta^2}}\left[C_2 + \frac{1}{\pi}⨍_{-1}^{1}\frac{\sqrt{1-\xi^2}}{\xi-\eta}\{g_n(\alpha\xi)-C_1\}\,d\xi\right] \tag{A12}$$

where the star on the integral sign means that we take its principal value. To find an expression for the constant C_1, we now define the function $I_n^{(1)}(\alpha\eta)$ according to

$$I_n^{(1)}(\alpha\eta) = \frac{1}{\pi}⨍_{-1}^{1}\frac{\sqrt{1-\xi^2}}{\xi-\eta}g_n(\alpha\xi)\,d\xi \tag{A13}$$

and rewrite (A12) in the form

$$F_n(\alpha\eta) = \frac{1}{\sqrt{1-\eta^2}}\left[C_2 + I_n^{(1)}(\alpha\eta) - C_1\frac{1}{\pi}⨍_{-1}^{1}\frac{\sqrt{1-\xi^2}}{\xi-\eta}d\xi\right]. \tag{A14}$$

The derivation of the integral on the right-hand side of (A14) can be found in [7] (and from now on will be assumed to be a known integral), so that we can write

$$F_n(\alpha\eta) = \frac{1}{\sqrt{1-\eta^2}}\left[C_2 + I_n^{(1)}(\alpha\eta) + C_1\eta\right]. \tag{A15}$$

We can now use (A15) and (A10) to write

$$C_1 = \frac{\hat{D}_n}{\tilde{D}} \tag{A16}$$

where

$$\hat{D}_n = \int_{-1}^{1} \frac{\eta I_n^{(1)}(\alpha\eta)}{\sqrt{1-\eta^2}\left[1+(\alpha\eta)^2\right]} d\eta \tag{A17}$$

$$\tilde{D} = \frac{\pi}{\alpha^2} - \int_{-1}^{1} \frac{\eta^2}{\sqrt{1-\eta^2}\left[1+(\alpha\eta)^2\right]} d\eta. \tag{A18}$$

Equation (A15) is, therefore, the *novel rigorous* inversion formula for the singular integral equation in (12).

Appendix II

The integrations that need to be performed to obtain the results shown in (39) through (48) are

$$I_n^{(1)}(\alpha\eta) = \frac{1}{\pi} \fint_{-1}^{1} \frac{\sqrt{1-\xi^2}}{\xi-\eta} g_n(\alpha\xi)\, d\xi \tag{A19}$$

$$I_m^{(2)}(\alpha\eta) = \int_{\eta}^{1} \frac{g_m^*(\alpha\xi)}{\left[1+(\alpha\xi)^2\right]} d\xi \tag{A20}$$

$$\tilde{D} = \frac{\pi}{\alpha^2} - \int_{-1}^{1} \frac{\eta^2}{\sqrt{1-\eta^2}\left[1+(\alpha\eta)^2\right]} d\eta \tag{A21}$$

$$D = \int_{-1}^{1} \frac{d\eta}{\sqrt{1-\eta^2}\left[1+(\alpha\eta)^2\right]}. \tag{A22}$$

The first integration, namely (A19), is more conveniently carried out using a numerical rather than an analytical procedure. The other three integrals, namely (A20), (A21), and (A22), can be evaluated analytically. Before a numerical procedure can be applied to evaluate (A19), however, a few analytical manipulations are necessary since the integrand is singular for $\eta = \xi$. Furthermore, the function $g_n(\alpha\eta)$ defined in (19) can be divided into real and imaginary parts. As a result, the evaluation of (A19) actually involves the evaluation of two similar integrals; one for the real part and one for the imaginary part. Taking as an example the integration involving the real part, we first write, for $n \neq 0$,

$$\begin{aligned} I_{n,\text{real}}^{(1)} &= \frac{1}{\pi} \int_{-1}^{1} \frac{\sqrt{1-\xi^2}}{\xi-\eta} \cos\left[2n\sin^{-1}(\alpha\xi)\right] d\xi \\ &= \frac{1}{\pi} \int_{-1}^{1} \frac{(1-\xi^2)\cos\left[2n\sin^{-1}(\alpha\xi)\right] - (1-\eta^2)\cos\left[2n\sin^{-1}(\alpha\eta)\right]}{\sqrt{1-\xi^2}(\xi-\eta)} d\xi \\ &\quad + (1-\eta^2)\cos\left[2n\sin^{-1}(\alpha\eta)\right] \cdot \frac{1}{\pi} \fint_{-1}^{1} \frac{d\xi}{\sqrt{1-\xi^2}(\xi-\eta)}. \end{aligned} \tag{A23}$$

The second integral on the right-hand side of (A23) can be found in [7] and is equal to zero for $|\eta| < 1$. The first integral on the right-hand side of (A23) is no longer singular for $\eta = \xi$ and can now be evaluated numerically. However, in view of the next integration required, namely (37), it is convenient to introduce the two changes of variable

$$\xi = \sin\left(\frac{\pi}{2}\psi\right) \tag{A24}$$

$$\eta = \sin\left(\frac{\pi}{2}\phi\right). \tag{A25}$$

Using (A23), (A24), and (A25), we then obtain the expression shown in (43). Following a similar procedure we can also obtain the expression for $I_{n,\text{imag}}^{(1)}$ shown in (45). For the case $n = 0$ we have

$$I_{0,\text{real}}^{(1)} = \frac{1}{\pi} \fint_{-1}^{1} \frac{\sqrt{1-\xi^2}}{\xi-\eta} d\xi = -\eta, \qquad |\eta| < 1 \tag{A26}$$

$$I_{0,\text{imag}}^{(1)} = 0. \tag{A27}$$

The subsequent use of the change of variables shown in (A25) yields from (A26) the result shown in (44).

To show that $I_{n,\text{real}}^{(1)}$ is an odd function and that $I_{n,\text{imag}}^{(1)}$ is an even function, let us define $I(\eta)$ according to

$$I(\eta) = \frac{1}{\pi} \fint_{-1}^{1} \frac{\sqrt{1-\xi^2}}{\xi-\eta} \xi^n\, d\xi. \tag{A28}$$

Next, we rewrite (A28) in the form

$$I(\eta) = \frac{1}{\pi} \int_{-1}^{1} \sqrt{1-\xi^2} \frac{\xi^n - \eta^n}{\xi-\eta} d\xi + \eta^n \frac{1}{\pi} \int_{-1}^{1} \frac{\sqrt{1-\xi^2}}{\xi-\eta} d\xi. \tag{A29}$$

Now, note that

$$\frac{\xi^n - \eta^n}{\xi-\eta} = \sum_{k=0}^{n-1} \xi^k \eta^{n-1-k} \tag{A30}$$

so that

$$I(\eta) = \sum_{k=0}^{n-1} \eta^{n-1-k} \frac{1}{\pi} \int_{-1}^{1} \sqrt{1-\xi^2}\, \xi^k\, d\xi - \eta^{n+1}. \tag{A31}$$

The integral on the right-hand side of (A31) is not equal to zero only if k is even; therefore

$$I(\eta) = \sum_{k=0}^{[(n-1)/2]} \eta^{n-1-2k} \frac{1}{\pi} \int_{-1}^{1} \sqrt{1-\xi^2}\, \xi^{2k}\, d\xi - \eta^{n+1} \tag{A32}$$

where the square brackets on the upper limit of the summation indicate the largest integer smaller than or equal to $(n-1)/2$. It is now easy to see that if n is even $I(\eta)$ is an odd function and if n is odd $I(\eta)$ is an even function. Since $g_n(\alpha\eta)$ in (A19) can be expanded in a series of powers of x, the above proves that $I_n^{(1)}$ in (27) is even if $g_n(\alpha\eta)$ is odd and is odd if $g_n(\alpha\eta)$ is even.

To carry out the integration in (A20) we only need to operate the change of variables

$$\alpha\eta = \tan\phi \tag{A33}$$

that transforms (A20) into a known integral. Furthermore, the constant terms that result from the integration in (A20) cancel out when we carry out the algebraic operations needed to go from (30) to (38), thereby giving the results shown in (39) through (42).

The integration to evaluate D in (A22) can be easily carried out using the change of variables

$$\eta = \sin\phi \tag{A34}$$

so that (A22) reduces to a known integral giving the result shown in (47). For $\tilde{D}$ in (A21) we can write

$$\begin{aligned}\frac{\alpha^2}{\pi}\tilde{D} &= 1 - \frac{\alpha^2}{\pi}\int_{-1}^{1}\frac{\eta^2}{\sqrt{1-\eta^2}\left[1+(\alpha\eta)^2\right]}\,d\eta \\ &= 1 - \frac{1}{\pi}\int_{-1}^{1}\frac{d\eta}{\sqrt{1-\eta^2}} + \frac{1}{\pi}\int_{-1}^{1}\frac{d\eta}{\sqrt{1-\eta^2}\left[1+(\alpha\eta)^2\right]}\end{aligned} \tag{A35}$$

which is a sum of known integrals giving the result shown in (48).

References

[1] M. Guglielmi and A. A. Oliner, "Multimode network description of a planar periodic metal-strip grating at a dielectric interface—Part I: Rigorous network formulations," *IEEE Trans Microwave Theory Tech.*, vol. 37, pp. 534–541, Mar. 1989.

[2] M. Guglielmi and A. A. Oliner, "Multimode network description of a planar periodic metal-strip grating at a dielectric interface—Part II: Small-aperture and small-obstacle solutions," *IEEE Trans. Microwave Theory Tech.*, vol. 37, pp. 542–552, Mar. 1989.

[3] F. Oberhettinger, "*Fourier Expansions a Collection of Formulas*. New York: Academic Press, 1973, p. 16.

[4] N. I. Muskhelishvili, "*Singular Integral Equations*, 2nd ed. Institute of Mathematics, Tiflis, U.S.S.R., 1946, p. 57.

[5] M. Abramowitz and I. A. Stegun, *Handbook of Mathematical Functions*. New York: Dover, 1970, pp. 916–917.

[6] G.L. Baldwin and A.E. Heins, "On the diffraction of a plane wave by an infinite plane grating," *Math. Scand.*, vol. 2, pp. 103–118, 1954.

[7] L. Lewin, *Theory of Waveguides*. New York: Wiley, 1975, p. 201.

Marco Guglielmi was born in Rome, Italy, on December 17, 1954. He received the degree "Laurea in Ingegneria Elettronica" in 1979 from the University of Rome "La Sapienza," Rome, Italy, where in 1980 he also attended the "Scuola di Specializzazione in Elettromagnetismo Applicato". In 1981 he was awarded a Fulbright Scholarship in Rome, Italy, and an HISP scholarship (Halsey International Scholarship Program) from the University of Bridgeport, Bridgeport, CT, where in 1982 he obtained the M.S. degree in electrical engineering. In 1986 he received the Ph.D. degree in electrophysics from Polytechnic University, Brooklyn, NY.

From 1984 to 1986 he was an Academic Associate at Polytechnic University and since 1986 he has been an Assistant Professor in the Electrical Engineering Department there. In 1987 he was the second prize winner of the URSI National Student Paper Prize Competition in Boulder, CO. His professional interests include the areas of solid-state devices and circuits, microwave active and passive devices, network representations of waveguide discontinuities, periodic structures, phase arrays, and millimeter-wave leaky-wave antennas.

Harry Hochstadt was born in Vienna, Austria, on September 7, 1925. He emigrated to the United States in 1938, where he has resided since. In 1949, he obtained the degree of bachelor of chemical engineering from Cooper Union. In 1950 he was awarded the M.S. degree in mathematics and in 1956, the Ph.D. degree in Mathematics, both from the Courant Institute.

From 1951 through 1957, he worked as a Research Engineer for the W. L. Maxson Corporation. In 1957, he joined the Polytechnic Institute of Brooklyn, Brooklyn, NY, as Assistant Professor of Mathematics. Currently, he holds the position of Professor of Mathematics and Head of Department at the same institution, now known as Polytechnic University. His professional interests include different areas of applied mathematics such as differential equations and differential operator theory, in particular, as applied to inverse spectral problems.

Dr. Hochstadt is the author of numerous textbooks involving special functions, ordinary differential equations, and integral equations.